ФИЗИКА ТВЕРДОГО ТЕЛА И КОНДЕНСИРОВАННЫХ СРЕД

ERD STUDIES OF D-ION DEPTH DISTRIBUTIONS AFTER IMPLANTATION INTO SOME PURE METALS AND ALLOYS

A. Yu. Didyk [a, 1], *R. Wiśniewski* [b, 2],
T. Wilczynska [b], *K. Kitowski* [b], *A. Hofman* [b]

[a] Joint Institute for Nuclear Research, Dubna

[b] Institute of Atomic Energy POLATOM, Otwock/Świerk, Poland

This paper presents a report on experimental results of depth distributions of deuterium ions implanted with 25 keV energy at a fluence interval of $(1.2-2.3) \cdot 10^{22}$ m^{-2} into samples of pure metals (Cu, Ti, Zr, V, Pd) and diluted Pd alloys (Pd–Ag, Pd–Pt, Pd–Ru, Pd–Rh). The post-treatment depth distributions of deuterium and hydrogen atoms were measured within a few hours after implantation with the use of elastic recoil detection (ERD) analysis. After three months the measurements were repeated. The comparison of the obtained results in both series of studies allowed us to make an important observation of the desorption rates of implanted deuterium atoms from pure metals and diluted Pd alloys. The maximum measured concentrations of deuterium atoms in pure Zr and Ti foils with relatively small desorption rate of deuterium atoms within three months after implantation were observed. Also a very high spreading of deuterium atom distributions was observed in all the measured pure metals and alloys. It can be explained by the large diffusion coefficients of deuterium and extremely fast kinetics.

В работе представлены экспериментальные результаты по определению распределения ионов дейтерия, имплантированных при энергии 25 кэВ в диапазоне флюенсов $(1,2-2,3) \cdot 10^{22}$ м$^{-2}$ в образцы чистых металлов (Cu, Ti, Zr, V, Pd) и разбавленные сплавы Pd (Pd–Ag, Pd–Pt, Pd–Ru, Pd–Rh). Распределения атомов дейтерия по глубине были изучены с применением метода регистрации ядер отдачи практически непосредственно после имплантации. Спустя три месяца измерения были повторены. Сравнение полученных результатов в обеих сериях измерений позволило сделать важные заключения о скоростях десорбции имплантированного дейтерия из вышеперечисленных металлов и сплавов Pd. Через три месяца после имплантации установлены максимальные концентрации имплантированного дейтерия в фольгах из Zr и Ti, а также относительно невысокие скорости его десорбции. Показано, что во всех имплантированных дейтерием образцах наблюдается значительное перераспределение атомов дейтерия по глубине. Это объясняется экстремально высокими коэффициентами диффузии и быстрой кинетикой процессов в ряде измеренных материалов.

PACS: 25.45.-z

---

[1] E-mail: didyk@jinr.ru

[2] E-mail: roland.wisniewski@gmail.com

INTRODUCTION

Limited energy resources and pollution increase associated with energy production have stimulated the search for cleaner, cheaper, and more efficient technologies. One promising technology involves hydrogen stored in metal hydrides [1, 2].

Hydrogen and its heavier isotopes serve as a nuclear fuel in fusion reactor power stations [3]. They are also utilized widely in currently operative nuclear reactors for slowing neutrons down, but also as reflectors-mirrors of neutrons, as safety materials, and in the regulatory systems [4].

The basic challenge in all these applications and in the promising future ones would be to obtain as high as possible concentration of hydrogen in storage-accumulators while creating relatively simple conditions for hydrogen desorption in hydrogen energetics [4] and possibly in future mobile-engine applications [2].

One of the informative methods of investigating the hydrogen and its heavy isotope behavior is elastic recoil detection (ERD) analysis, which allows one to get information about migration, diffusion, storage and desorption processes under implantation [3].

The purpose of this article is to present a report on experimental data of depth distributions of D and H atoms in metals and alloys after implantation of D^+ ions up to high fluences. Time stability of such implanted layers and desorption rates of implanted D^+ ions are another important concern of the study (see [5] and references therein).

1. EXPERIMENTAL METHODS AND RESULTS

All the used samples had a purity of about 99.9% and sizes $10 \times 15 \times 0.2$ mm. They had not been outgassed before implantation, just for some alloys the initial concentration of hydrogen was measured (see Table 2, Part 1). The implantation of D^+ ions with an energy of 25 keV was carried out on a special setup based on the electron cyclotron resonance ion source (ECR) at the Flerov Laboratory of Nuclear Reactions. Homogeneity of irradiation with the use of two scanning systems on a square of about 6×4 cm was $\pm 2-3\%$ and the temperature of implantation was $\sim 30°C$. Samples of metals and alloys were irradiated up to four D^+-ion fluences: $1.2 \cdot 10^{22}$, $1.5 \cdot 10^{22}$, $1.8 \cdot 10^{22}$, and $2.3 \cdot 10^{22}$ m^{-2}.

Please be advised that all implanted metal samples (V, Zr, Ti, and Pd) were deformed by a spontaneous emergence of gas pores or gas bubbles, i.e., swelling processes (see [3, 5] and references therein). There was a surface discoloration with intensity depending on the D^+-ion implantation fluence. This phenomenon is different from the optical phenomenon caused by the switchable mirrors which was described (see, for example, [6, 7]) for yttrium or other thin rare-earth metal layers.

ERD studies [8] were carried out with He$^+$ ions with an energy of 2.3 or 1.9 MeV, and the obtained experimental spectra were then modeled with the help of computer code SIMNRA6.05.

The depth-dependent concentrations of D and H atoms at two fluences of implantations $1.5 \cdot 10^{22}$ and $2.3 \cdot 10^{22}$ m^{-2} for Zr samples are presented in Fig. 1. The projected range of D^+ ions in Zr foil is equal to $R_p^D = (1923 \pm 643)$ Å. The projected ranges of ERD-analyzed samples of He$^+$ ions (2.3 and 1.9 MeV) are in the interval
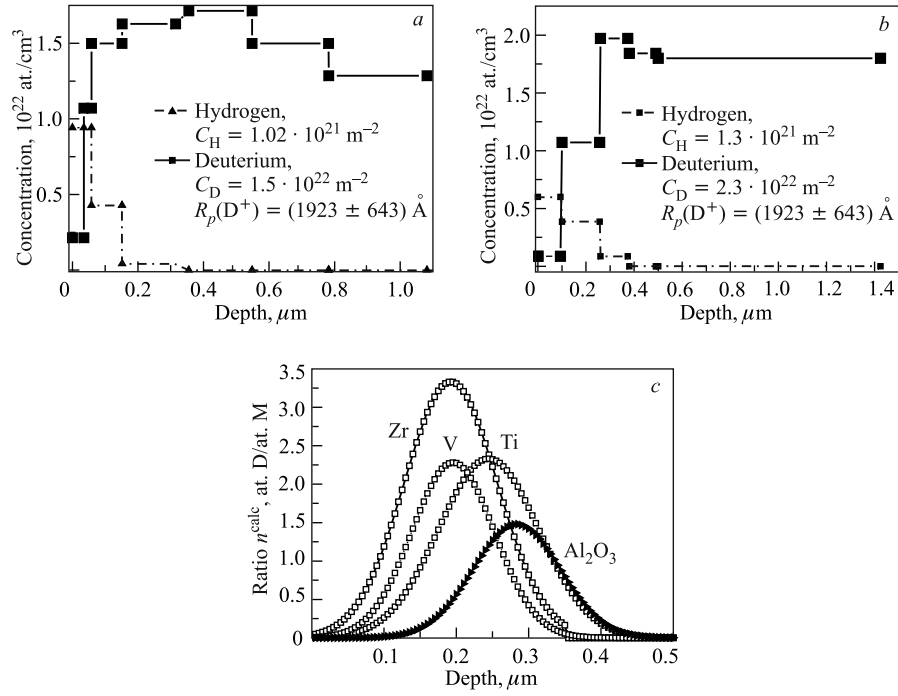
Fig. 1. The depth concentrations of D and H atoms after D^+-ion implantation with an energy of 25 keV at two fluences: $1.5 \cdot 10^{22}$ m^{-2} (*a*) and $\Phi_{\max} = 2.3 \cdot 10^{22}$ m^{-2} (*b*) in Zr samples and calculating depth-dependent ratios (n^{calc}) for the studied materials corresponding to the maximum fluence (*c*)

from $R_p^{\mathrm{He}} \approx 0.9$ μm up to $R_p^{\mathrm{He}} \approx 1.5$ μm for the studied materials. Calculation of the projected range of distribution of the implanted ions was performed using the TRIM-2007 computer code [9]. The integral doses of D and H atoms in analyzing layers with the depths $Z < R_p^{\mathrm{He}}$ were used for estimations of storage and desorption effects of D atoms from all the studied samples after implantation. The observed large depth spread of implanted D^+ ions is connected with fast temperature diffusion and radiation-stimulated processes [3].

The sputtered surface layer thickness ΔZ under implantation of D^+ ions at the maximum ion fluence $\Phi_{\max} = 2.3 \cdot 10^{22}$ m^{-2} with sputtering coefficient $S_{\mathrm{Zr}} = 1.69 \cdot 10^{-3}$ at. Zr/ion D^+ is equal to $\Delta Z = \Phi_{\max} \cdot S_{\mathrm{Zr}}/N_{\mathrm{Zr}} \approx 10$ Å. One can conclude that the sputtering is negligibly small and such effects can be neglected in consideration in depth changes.

For calculating the ion profiles implanted into targets, the known formula (see [10]) was used:

$$C(Z) = \frac{N_0}{2 \times S} \left[\mathrm{erf}\left(\frac{Z + \dfrac{\Phi \times S}{N_0} - R_p^{\mathrm{D}}}{\sqrt{2} \times \Delta R_p^{\mathrm{D}}} \right) - \mathrm{erf}\left(\frac{Z - R_p^{\mathrm{D}}}{\sqrt{2} \times \Delta R_p^{\mathrm{D}}} \right) \right], \tag{1}$$

here N_0 is atomic target density; Φ is ion fluence; S is sputtering coefficient for target atoms; R_p^D and ΔR_p^D are projected range and straggling of ions in the target. The maximum ion depth concentration should be

$$C^{\mathrm{max}} = \frac{N_0}{S} \times \mathrm{erf} \left[\frac{\Phi \cdot S}{2\sqrt{2}N_0 \Delta R_p} \right] \tag{2}$$

at the respective depth $Z_{\mathrm{max}} = R_p - \dfrac{\Phi \cdot S}{2N_0}$. The curves of deuterium/metal ratios $n(Z) \equiv C(Z)/N_0$ versus depth are presented in Figs. 1, c and 4, b for the studied materials and respective D$^+$-ion fluences.

Figure 1 shows that: a) the depth concentrations of D atoms have a very big spread along the implanted ion path and the width of the implanted zone is much bigger than the projected range $Z > R_p^D = (1923\pm643)$ Å; b) the integral doses (C_D) of D atoms correspond closely to the experimental ion fluences for Zr targets only; c) the maximum value of the ratio obtained for D atoms in Zr $n_{\mathrm{Zr}}^{\mathrm{max}} = 0.90\,\mathrm{at.\,D/at.\,Zr}$ is significantly smaller than the calculated maximum value obtained using expressions (1) and (2): $n_{\mathrm{Zr}}^{\mathrm{max}}(D) \approx 3.3\,\mathrm{at.\,D/at.\,Zr}$ (see Fig. 1, c). The large spread of depth distributions of implanted and diffused deuterium atoms does not allow comparison of the calculated and experimental dependences in depth. This is a reason of introducing of integral D-atom doses.

For a comparative analysis the integral dose of D$^+$ ions implanted into the good-quality surface of Al$_2$O$_3$ single crystal is reported in Fig. 2. The projected range of D$^+$ ions in Al$_2$O$_3$ samples is equal to $R_p^D = (2832 \pm 602)$ Å (see also Fig. 1, c). The projected range of ERD-analyzed He$^+$ ions (2.3 MeV) is $R_p^{\mathrm{He}} = 1.38\ \mu$m.

It is easy to see from Fig. 2 that: a) the depth distributions of implanted D$^+$ ions for fluence $\Phi_{\mathrm{max}} = 2.3 \cdot 10^{22}$ m^{-2} have a very big spread along the implanted ion path and the width of the implanted zone is much bigger than the projected range; b) the integral dose of D atoms bigger than $C_D > 6.43 \cdot 10^{21}$ m^{-2} is still less than the previous results; c) the maximum measured depth concentration of D atoms in Al$_2$O$_3$ sample is about 15%,
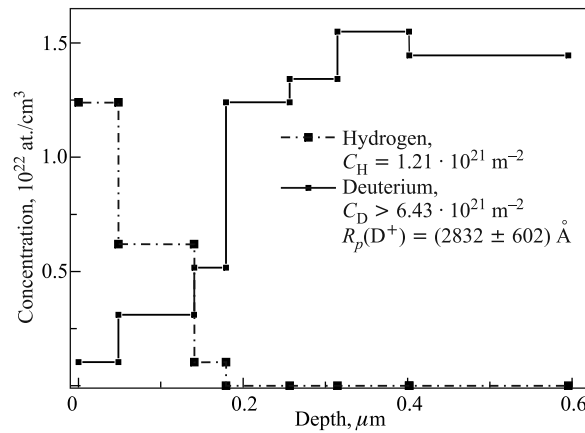

Fig. 2. The depth concentrations of D and H atoms after D$^+$-ion implantation with an energy of 25 keV at fluence $\Phi_{\mathrm{max}} = 2.3 \cdot 10^{22}$ m^{-2} in Al$_2$O$_3$ single crystal

i.e., $n_{Al_2O_3}^{exp} \cong 0.18$ at. D/at. $Al_2O_3 < n_{Al_2O_3}^{max} = 1.5$ at. D/at. Al_2O_3 (see Fig. 1, *c*). The maximum D-atom concentration was achieved at the depth levels from 0.26 to 0.4 μm. This depth area is comparable with the projected range of D^+ ions in Al_2O_3 sample.

The experimental D–Al_2O_3 low value ratio can be explained by a high spread of implantation layer, bigger than the analyzed He^+-ion projected range. It would be better to check this conclusion by another method for depth D-atom measurements, e.g., by secondary mass ion spectroscopy.

Also, the experimental results have been obtained under the ERD analysis of vanadium foils implanted by D^+ ions for all the studied fluences. The integral doses of D atoms in implanted V and Pd samples are presented in Figs. 3 and 4 for comparison. The projected ranges of D^+ ions and analyzed He^+ ions are $R_p^D = (1955 \pm 571)$ Å and $R_p^{He} = 1.04$ μm (for V), and $R_p^D = (1237 \pm 458)$ Å (see Figs. 1, *c* and 4, *b*) and $R_p^{He} = 0.9$ μm (for Pd). The calculated deuterium–V and deuterium–Pd ratios for implantation fluences $2.3 \cdot 10^{22}$ m^{-2} and $1.2 \cdot 10^{22}$ m^{-2} have values $n_V^{max}(D) \cong 2.3$ at. D/at. V and $n_{Pd}^{max}(D) \cong 1.5$ at. D/at. Pd, respectively (see Figs. 1, *c* and 4, *b*). The integral doses and depth concentrations of implanted D atoms are very low. The measured values of D-atom concentrations in both V and Pd
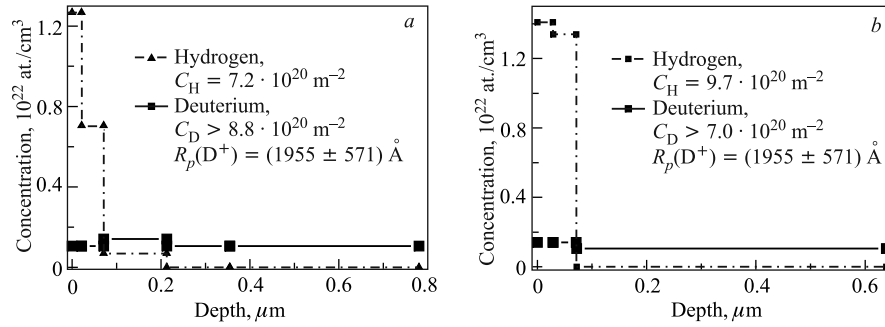

Fig. 3. The depth concentrations of D and H atoms after D^+-ion implantation with an energy of 25 keV at two fluences: $1.5 \cdot 10^{22}$ m^{-2} (*a*) and $\Phi_{max} = 2.3 \cdot 10^{22}$ m^{-2} (*b*) in V samples
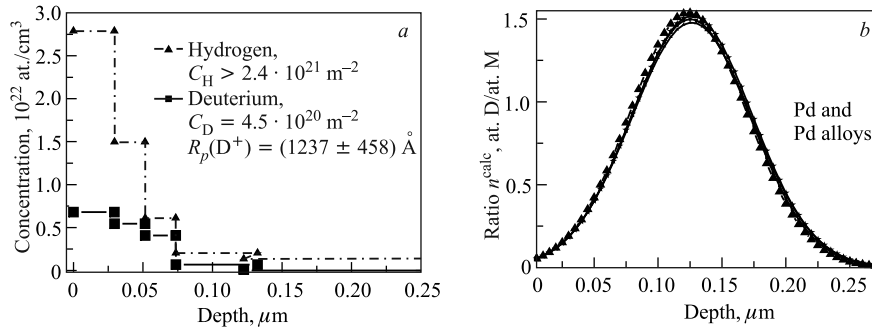

Fig. 4. The depth concentrations of D and H atoms after implantation of D^+ ions with an energy of 25 keV at fluence $1.2 \cdot 10^{22}$ m^{-2} in Pd sample (*a*) and depth-dependent ratios (n^{calc}) for Pd and Pd alloys (*b*)

implanted foils are about $< 1-2\%$ only; i.e., these values are near the minimum levels of ERD-analysis sensitivity.

It is known that Pd foils can be used as super filters of hydrogen isotopes and impenetrable membranes for other gases [4]. The conclusion of our studies, with respect to the previous results (see, for example, [6, 7, 11, 12]), is that thick V foils (0.2 μm thickness) can be used as selective membranes for cleaning of hydrogen isotopes from other gases. It is necessary to use also atomizer for partition of deuterium or hydrogen molecules into atoms. Let us present the room temperature diffusion coefficients of D atoms in thick V foils: $D_D = 2.2 \cdot 10^{-9}$ m^2/s [11], and for hydrogen diffusion in thin V foils is about $D_H = 1.6 \cdot 10^{-9}$ m^2/s [7].

The main difference between our results and the previous ones [7, 11, 12] is the following: in spite of high level of mechanical stress in D$^+$-ion implanted V foils (it is ensued from bended shape of implanted foils) and surfaces colors changes (Pd foil becomes dark blue and V dark brown), a low level of implanted deuterium concentrations and a large spread of depth profiles were observed. These results are also conflicted with the creation of high-pressure gas bubbles at high fluences [4, 10].

All experimentally measured values for D-atom integral doses in the studied materials (Zr, Ti, V, Cu, Pd, SS, and Al$_2$O$_3$) are presented in Table 1. It is valuable to note that the sputtered layers in all the studied metals and alloys are very narrow (about 10–20 Å) in comparison to the projected range of D$^+$ ions in them. As can be seen from Table 1, there is a close relation between the experimentally measured integral doses and the implanted ion fluences; besides, a big spread of experimental profiles is observed in metals and complex composed targets. Some empty positions in Table 1 are not filled yet and there are some inconsistencies to be settled in the very near future.

Table 1. **Integral doses of D atoms** $(10^{22}$ **m**$^{-2})$ **after implantation of D$^+$ ions in Zr, Ti, Cu, Pd, V metals, stainless steel, and Al$_2$O$_3$ single crystal at various fluences** Φ_D $(10^{22}$ **m**$^{-2})$

Materials implanted	Fluence of D$^+$-ion implantation $\Phi_D, 10^{22}$ m^{-2}			
	1.2	1.5	1.8	2.3
Zirconium, Zr	—	1.5	1.5	2.3
Titanium, Ti	—	—	0.6	0.7
Copper, Cu	—	0.29	—	—
Stainless steel, Fe$_{72}$Cr$_{18}$Ni$_{10}$	—	0.23	—	—
Al$_2$O$_3$	—	—	—	0.64
Palladium, Pd	0.05	—	—	—
Vanadium, V	—	0.09	0.04	0.07

The summary data of D- and H-atom integral doses measured before (in some cases), immediately after and in various time periods from D$^+$-ion implantation are presented in Table 2 (Part 1 and Part 2). As is shown, the maximum concentration of H atoms was measured in initial Zr foils in comparison with Al$_2$O$_3$ and Ti ones. And there is a decrease in D-atom integral doses in all implanted, up to high fluence $\Phi_{max} = 2.3 \cdot 10^{22}$ m^{-2}, measured samples (Al$_2$O$_3$, Zr, Ti, and V). The maximum decrease for all the measured materials is about 3–4 times less.

This result contradicted the results of creation of H, D and He gas bubbles and bubble lattices at high fluence of implantation (see [5, 10]). It is necessary to check again such different behavior after a long period of implantation.

Table 2. **Integral doses of D and H atoms** (10^{22} m^{-2}) **before and after implantation of** D^+ **ions at fluence** $2.3 \cdot 10^{22} \text{ m}^{-2}$ **and after three months for the studied metals (Zr, Ti, V) and** Al_2O_3 **(Part 1) and integral doses of D and H atoms** (10^{22} m^{-2}) **in palladium alloys** ($Pd_{0.9}Ag_{0.1}$, $Pd_{0.9}Pt_{0.1}$, $Pd_{0.9}Ru_{0.1}$, **and** $Pd_{0.9}Rh_{0.1}$) **at fluence** $1.2 \cdot 10^{22} \text{ m}^{-2}$ **(Part 2) after two months**

Part 1						
Materials		Al_2O_3	Zr	Ti	V	
Hydrogen	Initial samples	0.049	0.21	0.069	—	
Deuterium	Measurements of samples implanted by 25-keV D^+ ions at fluence $2.3 \cdot 10^{22} \text{ m}^{-2}$, ERD analysis by He^+ (2.3 MeV) ions after implantation	0.64	2.3	0.54	0.097	
				0.66	0.070	
Hydrogen		0.12	0.13	0.06	0.06	
		0.15	0.11		0.06	
Deuterium	Measurements of samples implanted by 25-keV D^+ ions at fluence $2.3 \cdot 10^{22} \text{ m}^{-2}$, ERD analysis by He^+ (1.9 MeV) ions three months after implantation	0.15	0.65	0.16	0.02	
Hydrogen		0.16	0.27	0.13	0.09	
Part 2						
Materials		Pd	$Pd_{0.9}$ $Ag_{0.1}$	$Pd_{0.9}$ $Pt_{0.1}$	$Pd_{0.9}$ $Ru_{0.1}$	$Pd_{0.9}$ $Rh_{0.1}$
Deuterium	Measurements of samples after D^+-ion implantation at fluence $1.2 \cdot 10^{22} \text{ m}^{-2}$,	0.05	0.03	0.03	0.03	0.03
Hydrogen	ERD analysis by He^+ (2.3 MeV) ions after implantation	0.24	0.17	0.16	0.24	0.32
Deuterium	Measurements of samples implanted by 25-keV D^+ ions at fluence $1.2 \cdot 10^{22} \text{ m}^{-2}$,	—	0.02	0.03	0.03	0.02
Hydrogen	ERD analysis by He^+ (1.9 MeV) ions two months after implantation	—	0.11	0.10	0.07	0.11

The complete ERD measurement results of integral D- and H-atom doses at Pd and some palladium alloys, such as $Pd_{0.9}Ag_{0.1}$, $Pd_{0.9}Pt_{0.1}$, $Pd_{0.9}Ru_{0.1}$, and $Pd_{0.9}Rh_{0.1}$, are presented in Table 2 (Part 2). Comparison of the experimental results presented in Tables 2 and 1 shows that the integral doses of implanted D atoms and existing integral concentrations of H atoms do not change much for a long period (two months) between measurements. Some differences are most probably related to different equipment setups used for ERDA study and differing energies of used He^+-ion beams. It is necessary to note that depth distributions of H atoms are very deep and have high integral dose values for all Pd alloys. The conclusion is that both components, D atoms and H atoms, do not participate in desorption processes and exist in alloy lattices as gas atoms absorbed and trapped, i.e. mainly as substitutive impurities, or in small gas bubbles (see [5, 10]). The achieved integral concentrations of hydrogen atoms are high at $(1.5-3.2) \cdot 10^{21} \text{ m}^{-2}$, which is very promising for possible future applications of that type of energy storage. The depth distributions of H atoms have a wide spread at big depth from surfaces for all the studied Pd alloys.

CONCLUSION

It was shown that the measured integral concentrations of D atoms for all the fluences $(1.5 \cdot 10^{22}, 1.8 \cdot 10^{22}, \text{ and } 2.3 \cdot 10^{22} \text{ m}^{-2})$ of D^+-ion implantations in Zr, Ti, Cu, SS, and Al_2O_3 correspond to ion fluences, particularly for Zr. The observed depth dependency of D atoms has a spreading tendency along the projected range of D^+ ions.

D^+-ion implantation up to superhigh fluences with small used ion flux $\approx 3.5 \cdot 10^{17} \text{ m}^{-2} \cdot \text{s}^{-1}$ allowed one to get high concentrations and integral doses in most of the studied metals and alloys, excluding V and Pd samples. D-atoms saturated layers have a very large width in depth (spread layer) much bigger than the D^+-ion projected ranges and without blistering and flaking processes.

Desorption was observed to occur in all the studied metals such as Zr, Ti and Al_2O_3 single crystal. As is well known [5, 10], the H and He ions implanted into Ni foils at fluence interval 10^{17}–10^{18} cm^{-2} should mainly be in lattice of gas bubble with atomic helium gas density $\sim 2 \cdot 10^{23}$ He/cm^3 at very high pressure, about 50 GPa, and in solid state (see [10, p. 175]).

It was established that there was a very high desorption of deuterium ions from implanted vanadium samples for all the used implantation fluences. The comparison of V and Pd implanted samples allows one to conclude that V foils can be used together with more expensive Pd foils for separation and purification of hydrogen and its heavier isotopes from other gases. It is just possible with the use of so-called atomizers.

REFERENCES

1. *Winter C. J., Nitsch J.* Hydrogen as an Energy Carrier: Technologies, Systems, Economy. Springer, 1988.
2. *Schlapbach L., Zuttel A.* Hydrogen-Storage Materials for Mobile Applications // Nature. 2001. V. 414. P. 353–361.
3. *Chernov I. P. et al.* Hydrogen Migration in Stainless Steel and Titanium Alloys, Stimulation by Ionizing Radiation // J. Nucl. Mat. 1996. V. 233–237. P. 1118–1122.
4. Metal Hydrides as Materials of Nuclear Reactions / Eds. Mueller W. M., Blackledge J. P., Libowitz G. G. N. Y.; London, 1968. P. 58–83.
5. *Kalin B. A., Chernov I. I.* Lattice Organization of Pore and Bubble Structure in Irradiated Metals and Alloys // Atomic Science Abroad. 1986. V. 10. P. 3–9.
6. *den Broeder F. J. A. et al.* Visualization of Hydrogen Migration in Solids Using Switchable Mirrors // Nature. 1998. V. 394. P. 656–658.
7. *Vece M. Di., Remhof A., Kelly J. J.* Electrochemical Study of Hydrogen Diffusion in Vanadium Thin Film // Electrochem. Commun. 2004. V. 6. P. 17–21.
8. *Hrubčin L. et al.* Application of the ERD Method for Hydrogen Determination in Silicon (Oxy)Nitride Thin Films Prepared by ECR Plasma Deposition // Nucl. Instr. Meth. B. 1994. V. 85. P. 60–62.
9. *Ziegler J. F.* SRIM-2003 // Nucl. Instr. Meth. B. 2004. V. 219–220. P. 1026-1036; http://www.srim.org.
10. *Komarov F. F.* Ion Implantation into Metals. M.: Metallurgy, 1990. 216 p. (in Russian).
11. *Orimo Shin-ichi, Kimmerle F., Mayer G.* Hydrogen in Nanostructured Vanadium–Hydrogen Systems // Phys. Rev. B. 2001. V. 63. P. 094307-1–094307-10.
12. *Qi Zh. et al.* Tritium Diffusion in V, Nb and Ta // J. Phys. F. 1983. V. 13. P. 2053–2062.